



# CHORUS

This is the accepted manuscript made available via CHORUS. The article has been published as:

## Flat Bands and Giant Light-Matter Interaction in Hexagonal Boron Nitride

C. Elias, G. Fugallo, P. Valvin, C. L'Henoret, J. Li, J. H. Edgar, F. Sottile, M. Lazzeri, A. Ouerghi, B. Gil, and G. Cassabois

Phys. Rev. Lett. **127**, 137401 — Published 23 September 2021

DOI: [10.1103/PhysRevLett.127.137401](https://doi.org/10.1103/PhysRevLett.127.137401)

# Flat bands and giant light-matter interaction in hexagonal boron nitride

C. Elias,<sup>1</sup> G. Fugallo,<sup>2</sup> P. Valvin,<sup>1</sup> C. L’Henoret,<sup>1</sup> J. Li,<sup>3</sup> J. H. Edgar,<sup>3</sup>

F. Sottile,<sup>4</sup> M. Lazzeri,<sup>5</sup> A. Ouerghi,<sup>6</sup> B. Gil,<sup>1</sup> G. Cassabois<sup>1,\*</sup>

<sup>1</sup>Laboratoire Charles Coulomb UMR 5221 CNRS-Université de Montpellier, 34095 Montpellier, France

<sup>2</sup>LTeN UMR 6607 CNRS-PolytechNantes, Université de Nantes, 44306 Nantes, France

<sup>3</sup>Tim Taylor Department of Chemical Engineering,

Kansas State University, Manhattan Kansas 66506, USA

<sup>4</sup>Laboratoire des Solides Irradiés, Ecole Polytechnique, CNRS,

CEA/DRF/IRAMIS, Institut Polytechnique de Paris, 91128 Palaiseau, France

<sup>5</sup>Sorbonne Université, CNRS UMR 7590, MNHN, IMPMC, 75005 Paris, France

<sup>6</sup>C2N CNRS-Univ Paris Sud, Université Paris-Saclay, 91120 Palaiseau, France

(Dated: September 1, 2021)

Dispersionless energy bands in  $k$  space are a peculiar property gathering an increasing attention for the emergence of novel electronic, magnetic and photonic properties. Here, we explore the impact of electronic flat bands on the light-matter interaction. The van der Waals interaction between the atomic layers of hexagonal boron nitride induces flat bands along specific lines of the Brillouin zone. The macroscopic degeneracy along these lines leads to van Hove singularities with divergent joint density of states, resulting in outstanding optical properties of the excitonic states. For the direct exciton, we report a giant oscillator strength with a longitudinal-transverse splitting of 420 meV, a record value, **confirmed by our *ab initio* calculations**. For the fundamental indirect exciton, flat bands result in phonon-assisted processes of exceptional efficiency, that compete with direct absorption in reflectivity, and that make the internal quantum efficiency close to values typical of direct bandgap semiconductors.

Flat-band engineering is the subject of intense research for investigating strongly-correlated states in systems made of electrons, cold atoms and photons [1]. **From a curiosity in magnetic frustration, flat bands have become a key fingerprint sought for in synthetic devices for studying superconductivity arising from electronic interactions, correlated insulator states, spontaneous ferromagnetism and quantum Hall effect [2–4]. Flat bands exist naturally in materials such as bulk van der Waals insulators, hexagonal boron nitride (hBN) being a model example. With the advent of graphene and transition metal dichalcogenides, hBN has become a key compound in 2D materials research, with the usual indirect-direct crossover of the bandgap at the monolayer limit [5–8]. However, there is also a rich physics in the bulk form of hBN, with original photonic properties that have been only recently explored [9].**

In this Letter, we report giant light-matter interaction arising from electronic flat bands in **bulk hBN. In addition to the weak interlayer interaction typical of Van der Waals structures, the ionicity difference between B and N enhances localization effects, resulting in electronic flat bands along specific Brillouin zone lines parallel to the c-axis.** The macroscopic degeneracy along these lines leads to van Hove singularities with divergent joint density of states, resulting in unique optoelectronic signatures. The combination of reflectivity and photoluminescence (PL) experiments in state-of-the-art hBN crystals allows us to characterize direct and indirect excitons and compare our results to **a phenomenological model and** first-principles calcula-

tions. For the direct exciton, we report a giant oscillator strength with a longitudinal-transverse splitting of 420 meV, the highest value ever reported. For the fundamental indirect exciton, flat bands translate in highly efficient phonon-assisted processes, that compete with direct absorption in reflectivity, and that make the internal quantum efficiency close to values typical of direct bandgap semiconductors.

Bulk hBN is a layered material considered the insulating analog of graphite and known as "white graphite". The fundamental bandgap of  $\sim 6$  eV is indirect in bulk hBN with a minimum of the conduction band at the M point and a maximum of the valence band around K [Fig.1(a)]. There is a direct bandgap at the K point [Fig.1(a)], slightly higher in energy than the indirect one. Excitonic effects are huge in hBN with a binding energy of  $\sim 0.7$  eV [10–12]. In order to take into account the electron-hole interaction in the evaluation of the dielectric function  $\epsilon_{\mathbf{q},\omega}$  one has to solve the Bethe-Salpeter equation [13]. The solution is most often written in a basis of independent-particle transitions  $t$  of oscillator strengths  $\rho$  mixed by the exciton wavefunctions  $A_t^\lambda$ :

$$\epsilon_{\mathbf{q},\omega} \propto \sum_{\lambda} \frac{|\sum_t A_t^\lambda \rho^t(\mathbf{q})|^2}{\hbar\omega - E_\lambda + i\eta} \quad (1)$$

where  $t = vc$  labels a transition between a valence state  $v$  and a conduction one  $c$  and the sum runs over the  $\lambda$  excitons with wavevector  $\mathbf{q}$  (see Supplemental Material [14], Section *Ab initio calculations*). In the independent-particle approximation (IPA), the dielectric function is

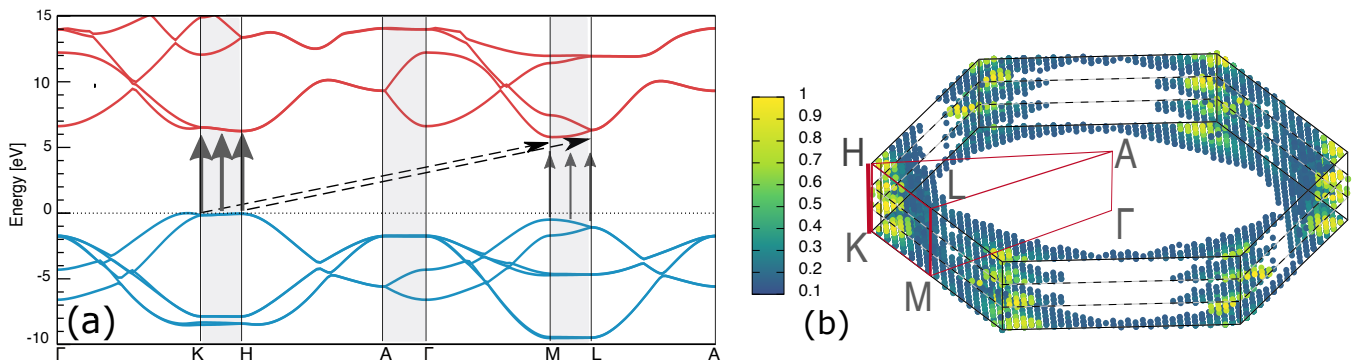


FIG. 1. (a) Electronic bandstructure evaluated in the framework of many-body GW calculations. The shaded areas indicate the paths that are parallel to the  $c$ -axis in the Brillouin zone of bulk hBN. Arrows in dark grey (dashed black) indicate the parallel direct (indirect) transitions contributing to the formation of the direct ( $dX$ ) and indirect ( $iX$ ) excitons, respectively. (b) Color map in the Brillouin zone of bulk hBN of the weighted oscillator strengths  $A_{\lambda}^t \rho^t(\mathbf{q})$  [as defined in Eq.(1)] building the  $dX$  exciton. For the sake of clarity, the map is limited to the points of the prevailing direct independent-particle transitions  $t$ , that contribute in total to 80% of the  $dX$  absorption. The irreducible part of the Brillouin zone is delimited by red lines, which are thicker for the KH and ML paths.

given by the simple expression:

$$\epsilon_{\mathbf{q},\omega}^{(\text{IPA})} \propto \sum_t \frac{|\rho^t(\mathbf{q})|^2}{\hbar\omega - E_t + i\eta} \quad (2)$$

In the absence of electron-hole interaction [Eq.(2)], the optical resonances are governed, in a first approximation, by the optical matrix elements and the joint density of states. In the case of flat bands, the joint density of states presents van Hove singularities that stem from the large number of transitions contributing in parallel to a given optical resonance.

With the electron-hole interaction [Eq.(1)], the dielectric function is not only influenced by the van Hove singularities due to flat bands but also by the formation of the excitonic states. The products  $A_{\lambda}^t \rho^t(\mathbf{q})$  can be called "weighted oscillator strengths" and the total intensity of the exciton peak is determined by the constructive coherent superposition of these terms [Eq.(1)]. By examining the first-order correction to the  $A_t^{\lambda}$  wavefunctions:

$A_t^{\lambda} \sim \sum_{t'} \frac{W_{t'}^{\lambda}}{E_t - E_{t'}}$ , one observes that large terms arise from independent-particle transitions where the energy difference  $E_t - E_{t'}$  is small. Excitonic effects are therefore enhanced when mixing many independent-particle transitions with similar energy [40]. Besides the existence of van Hove singularities, this phenomenon further contributes to the emergence of outstanding optical properties in systems with flat bands.

The vertical and tilted arrows in Fig.1(a) indicate all the transitions contributing to the formation of the direct ( $dX$ ) and indirect ( $iX$ ) excitons in hBN, respectively [7, 11, 41]. These independent-particle transitions come from regions of the Brillouin zone, parallel to the  $c$ -axis, where the valence and conduction bands are almost flat and parallel. The  $iX$  exciton results from indirect transitions moving in parallel along the  $c$ -axis from  $K \rightarrow M$  to  $H \rightarrow L$  [Fig.1(a)]. The  $dX$  exciton builds as a collective

excitation of the crystal involving all direct transitions along the KH and ML lines [Fig.1(a)], as discussed in Ref.[11, 42]. However, the most intense transitions [depicted in yellow in Fig.1(b)] come from points distributed around the KH line. It reveals the contributions coming from the ML region are in fact negligible with respect to KH where the bands are flatter.

We have performed measurements by reflectivity and PL in high-quality crystals. Because of the indirect bandgap of bulk hBN, PL in hBN probes the fundamental indirect exciton  $iX$  which has an energy  $E_{iX}=5.955$  eV [7]. The direct excitonic state  $dX$  lies at a higher energy than  $E_{iX}$  and it is expected to determine the optical response above the bandgap of hBN. The interplay between direct and indirect excitons in the optical properties of hBN remains an open issue because reflectivity and absorption experiments have been so far very limited in hBN. In the eighties, Hoffman *et al.* reported the first reflectivity measurements in hBN, from the mid infrared to the deep ultraviolet, but at room temperature and in low-quality crystals made of pyrolytic boron nitride [43]. Watanabe *et al.* extended the experiments to high-quality crystals [44, 45]. Although these measurements were performed at cryogenic temperatures, no significant advance followed in the interpretation of the complex excitonic structure close to the bandgap of hBN. Here, we have achieved reflectivity experiments at low temperature with a high spectral resolution, for samples fabricated by a process enabling the formation of large single crystals [Fig.2, inset] with a thickness of few micrometers (see Supplemental Material [14]). This experimental **achievement** has allowed to reveal the fine structure of the reflectivity spectrum around 6 eV. We provide a quantitative interpretation of our reflectivity and PL data and we show how electronic flat bands result in exceptional optical properties of the direct and indirect excitons in hBN.

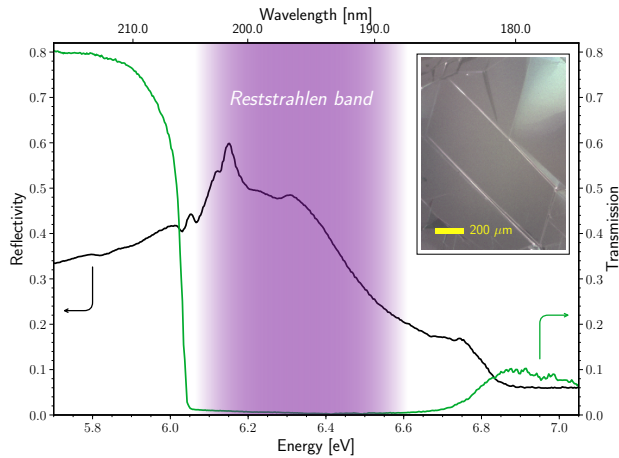


FIG. 2. Reflectivity (black) and transmission (green) of a high-quality hBN crystal, **recorded close to normal incidence** at 8K. The crystal thickness is  $4.5 \mu\text{m}$ . The shaded area indicates the excitonic reststrahlen band in hBN. Inset: microscope image of high-quality hBN synthesized by the metal flux method.

Reflectivity and transmission spectra in a  $4.5 \mu\text{m}$ -thick hBN crystal at 8K are plotted in Fig.2. The transmission drops abruptly around 6 eV and increases above noise level for energies larger than 6.6 eV. Such a spectrum is characteristic of the presence of a strong resonance above 6 eV. The spectral range of low-transmission is the so-called reststrahlen band, the general terminology used for vibrational and electronic resonances in solid state [46]. Although the present crystal is still too thick to extract the absorption spectrum in this energy range, the transmission spectrum in Fig.2 provides the spectral position of the excitonic reststrahlen band in hBN. We point out an unusually large value of its bandwidth of the order of half an eV, to be compared to few or tens of meV in standard semiconductors [46]. This is a first indication for the giant light-matter interaction and the existence of extremely large oscillator strengths in hBN. The reflectivity spectrum in Fig.2 displays previously unresolved fine structures. In particular, our measurements reveal the existence of four relative maxima of the reflectivity at 6.02, 6.05, 6.11 and 6.14 eV. The comparison with the PL spectrum in Fig.3 will show that they correspond to phonon-assisted optical transitions by the fundamental indirect exciton lying at  $E_{iX}=5.955$  eV. The observation of phonon-assisted absorption lines in the reflectivity spectrum of **an indirect** semiconductor is a unique feature without any equivalent example in the literature [46]. This is a second indication for the exceptional efficiency of the light-matter interaction in hBN, also stemming from the existence of electronic flat bands.

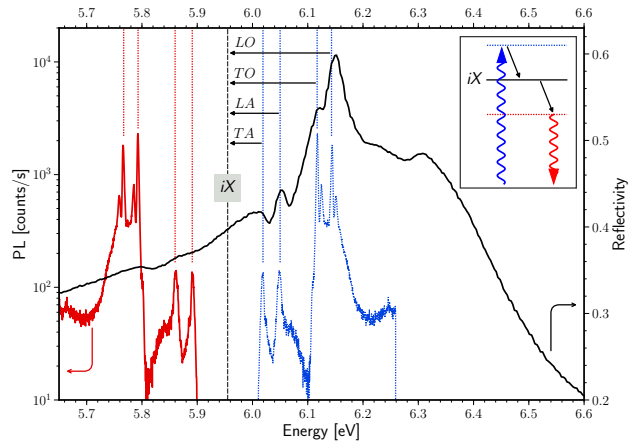


FIG. 3. Comparison between reflectivity (black) and photoluminescence (red) of bulk hBN at 8K. The vertical dashed line at 5.955 eV indicates the energy of the indirect exciton ( $iX$ ). The dotted blue spectrum corresponds to the mirror image of the PL spectrum with respect to the  $iX$  energy. Inset: schematic representation of absorption (blue) and emission (red) assisted by phonon emission (black arrow). The blue and red dashed lines indicate the virtual states involved in the phonon-assisted optical processes.  $TA$ ,  $LA$ ,  $TO$  and  $LO$  indicate the modes of the emitted phonons in reflectivity.

The indirect nature of the four lines detected in the reflectivity spectrum is demonstrated in Fig.3 where PL data are superimposed to the reflectivity spectrum. More precisely, the PL spectrum is displayed in solid red line while its mirror image with respect to the  $iX$  energy is shown in dotted blue line. Such a plot is motivated by the mirror symmetry between the processes of absorption and emission assisted by phonon emission in indirect semiconductors [46]: compared with the bandgap energy, photon emission is redshifted by the phonon energy, while photon absorption is blueshifted by the same value [as shown in the inset of Fig.3]. The comparison between the reflectivity spectrum and the mirrored PL one indicates that the four lines revealed by our reflectivity measurements are perfectly in resonance with the transitions due to phonon-assisted absorption in hBN. **From the assignment by PL spectroscopy [7] and in agreement with polarization selection rules [47]** the lines at 6.02, 6.05, 6.11 and 6.14 eV correspond to optical absorption assisted by the emission of one  $TA$ ,  $LA$ ,  $TO$  and  $LO$  phonon, respectively [Fig.3]. Such a phenomenology is in strong contrast to the textbook examples of phonon-assisted absorption. In standard semiconductors, indirect transitions appear as weak absorption bands which onset is difficult to identify [46, 48, 49], requiring either data post-processing [50] or modulation spectroscopy [46, 51]. In hBN, phonon-assisted absorption is readily observed with high contrast in reflectivity experiments, a unique situation among indirect semiconductors. We note that the existence of narrow lines rather

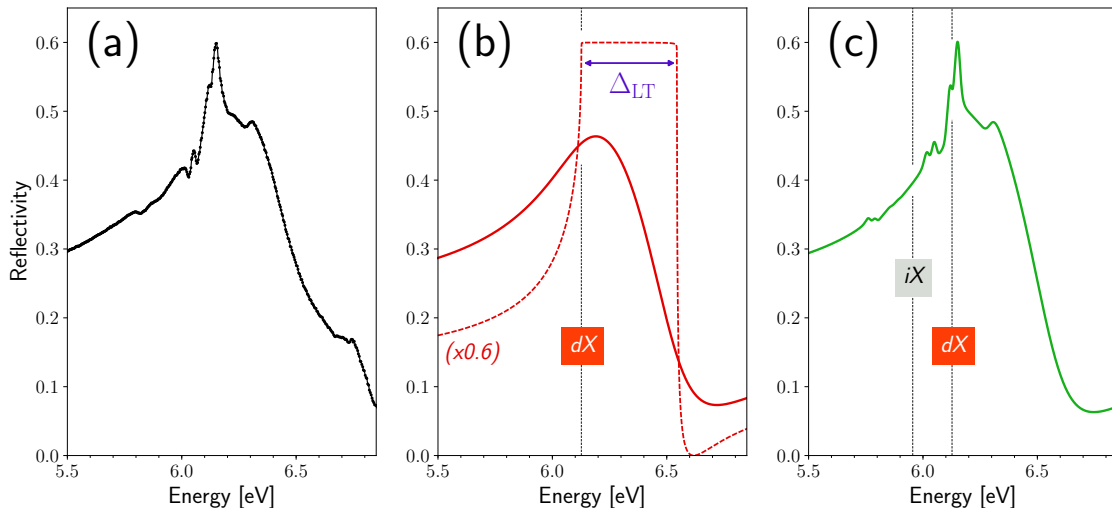


FIG. 4. (a) Experimental reflectivity spectrum at 8K. (b) Calculated reflectivity spectrum (red solid line) taking into account the direct exciton ( $dX$ ) only, with  $\gamma/\Delta_{LT}=0.41$  where  $\gamma$  is the  $dX$  linewidth and  $\Delta_{LT}$  is the longitudinal-transverse splitting.  $\Delta_{LT}=420$  meV in hBN. The red dashed line is the reflectivity spectrum calculated for  $\gamma/\Delta_{LT}=10^{-4}$  in order to better visualize  $\Delta_{LT}$ , which corresponds to the width of the reflectivity stop-band when  $\gamma/\Delta_{LT} \ll 1$ . (c) Calculated reflectivity spectrum (green solid line) taking into account the indirect ( $iX$ ) and direct ( $dX$ ) excitons ( $\gamma/\Delta_{LT}=0.41$ ).  $E_{iX}=5.955$  eV and  $E_{dX}=6.125$  eV.

than broad bands stems from the strong  $k$ -dependence of the exciton-phonon matrix element in hBN [7].

The experimental reflectivity spectrum [Fig.4(a)] is compared to the theoretical one calculated either with the optical transition of the direct exciton  $dX$  only [Fig.4(b)], or with both  $dX$  and  $iX$  contributions [Fig.4(c)] (see Supplemental Material [14], Section *Reflectivity modelling* for details on reflectivity calculations). The excellent agreement of our data with the calculated reflectivity spectrum in Fig.4(c) shows that we have reached a quantitative interpretation of the optoelectronic properties of hBN close to the bandgap. The direct exciton  $dX$  gives a broad pedestal fixing the order of magnitude of the reflectivity to  $\sim 50\%$  around 6 eV [Fig.4(b)]. The indirect exciton  $iX$  accounts for a series of narrow lines, that are phonon replicas decorating the smooth band of the direct exciton [Fig.4(c)]. We highlight the spectral coincidence of direct and indirect optical transitions in the near bandgap absorption of hBN. This peculiarity has so far hindered the comprehensive understanding of hBN physics [44, 52]. Our results unravel the complex interplay between direct and indirect processes in hBN, resulting in an unconventional optical response where the prominent peak at 6.1 eV does not arise from the direct exciton  $dX$  but from the indirect one  $iX$ .

From the quantitative interpretation of our experiments, we first comment the giant oscillator strength of the direct exciton  $dX$  due to electronic flat bands in hBN. For a given value of the excitonic linewidth, the higher the oscillator strength, the higher the reflectivity [53].

Conversely, for a given oscillator strength, the smaller the excitonic linewidth, the higher the reflectivity, as shown by the dashed line in Fig.4(b). In this limit, the reflectivity is of order unity in a spectral window corresponding to the so-called reststrahlen band. In complete analogy with optical phonons, the width of the excitonic reststrahlen band is given by the energy difference  $\Delta_{LT}$  between transverse and longitudinal exciton states [54, 55]. The longitudinal-transverse splitting  $\Delta_{LT}$  originates from Coulomb exchange interaction and it was shown that this exchange parameter can be remarkably expressed in a simple form as a function of the dipolar interaction matrix element [54, 55]. Therefore  $\Delta_{LT}$  is a common metric of the efficiency of the light-matter interaction. In hBN, we find  $\Delta_{LT}=420$  meV [Fig.4], the highest value ever reported in the literature to the best of our knowledge (see Supplemental Table 1 in the Supplemental Material [14]). Instructive is a first comparison with AlN. AlN shares many similarities with hBN but the lamellar structure. Both are nitride semiconductors with a similar bandgap of  $\sim 6$  eV, still  $\Delta_{LT}$  has a much lower value of 6 meV in AlN [56]. In hBN,  $\Delta_{LT}$  is enhanced by almost two orders of magnitude, a striking consequence of electronic flat bands. High values of  $\Delta_{LT}$  were reported in crystals with strongly bound excitons such as alkali halides [57, 58], solid neon and solid argon [59]. In these crystals,  $\Delta_{LT}$  follows the general scaling of the oscillator strength, that increases with the excitonic binding energy, and that is inversely proportional to the cube of the excitonic Bohr radius in the approximation of parabolic bands [60]. Usually, the more strongly bound the exciton is, the higher

$\Delta_{LT}$  [53, 56]. This standard rule in solid state is broken down because of the existence of flat bands. hBN provides an example of this effect, with exceptional degree as  $\Delta_{LT}$  surpasses any reported value in the literature, in particular the 360 meV in solid argon [59] which bandgap is  $\sim 14$  eV. This means the macroscopic degeneracy of the direct transitions along the KH line parallel to the c-axis [Fig.1(a)] has a dramatic impact on the optical properties of excitons in hBN, as illustrated by the ultralarge excitonic restrahten band [Fig.2] and the corresponding record value of  $\Delta_{LT}$  for the direct exciton  $dX$  [Fig.4(b)], **confirmed by** our first-principles calculations (see Supplemental Material [14], Section *Ab initio calculations*).

The light-matter interaction for the indirect exciton  $iX$  is radically different because of the coupling to the phonons field for satisfying the  $k$ -selection rule. Still, the parallel indirect transitions between the flat bands along the KH and ML lines [Fig.1(a)] play a key role in the optical properties of  $iX$ . From the quantitative interpretation of our data [Fig.4], one can analyze the effective oscillator strength of the phonon replicas identified from the comparison between PL and reflectivity [Fig.3]. For the optical phonon replicas ( $TO$  and  $LO$  lines), the effective oscillator strength is  $\sim 20$  times smaller than for  $dX$  (see Supplemental Material [14], Section *Reflectivity modelling* for details on reflectivity calculations). Such a reduction stems from the higher order of phonon-assisted optical transitions involving dipolar interaction and electron-phonon coupling. Still, the  $TO$  and  $LO$  replicas in hBN have an oscillator strength equivalent to direct materials with a longitudinal-transverse splitting of order 20 meV. The latter value is higher than  $\Delta_{LT}$  in direct wide bandgap semiconductors such as GaN, AlN and ZnO, where  $\Delta_{LT}=0.8, 6$  and  $11$  meV, respectively [56]. This means electronic flat bands in hBN

make phonon-assisted optical transitions stronger than direct ones in materials used in the optoelectronics industry [61, 62]. It also shows that the outstanding properties of indirect transitions in hBN are intrinsic, readily imprinted in the dielectric constant and observable in reflectivity and absorption experiments. As a consequence, this phenomenon also contributes to reaching an internal quantum efficiency of order unity in hBN [44, 52]. The intrinsic radiative processes bypass the extrinsic non-radiative ones in hBN, **and they occur in a few tens of ps** [63], because of the high oscillator strength due to electronic flat bands rather than because of the strong exciton-phonon coupling, as previously suggested [64]. Fifteen years after the pioneering work of Watanabe *et al.* [44], we thus unveil the physics behind the intense emission in hBN.

Our results bridge the fundamental physics of flat bands with applications where the giant light-matter interaction emerges as a resource for improved performances in optoelectronic devices. Moreover, our work opens exciting perspectives in cavity quantum electrodynamics by showing the possibility to couple photonic modes to excitonic states with an ultralarge oscillator strength in systems with flat bands.

#### Acknowledgments

We gratefully acknowledge P. Vuong for fruitful discussions. This work and the PhD funding of CE were financially supported by the network GaNeX (ANR-11-LABX-0014) and the BONASPES project (ANR-19-CE30-0007). JL and JHE are grateful for support from the Office of Naval Research, award number N00014-20-1-2474, for the hBN crystal growth. This work was performed using HPC resources from GENCI-[TGCC/CINES/IDRIS] within Project No. 100834.

\*e-mail: guillaume.cassabois@umontpellier.fr

- 
- [1] D. Leykam, A. Andreanov, and S. Flach, *Adv. Phys. X* **3**, 1473052 (2018).
  - [2] Y. Cao *et al.*, *Nature* **556**, 80-84 (2018).
  - [3] L. Balents, C. Dean, D.K. Efetov and A.F. Young, *Nat. Phys.* **16**, 725-733 (2020).
  - [4] G. Chen *et al.*, *Nature* **579**, 56-61 (2020).
  - [5] K.F. Mak, C. Lee, J. Hone, J. Shan, and T.F. Heinz, *Phys. Rev. Lett.* **105**, 136805 (2010).
  - [6] G. Wang *et al.*, *Rev. Mod. Phys.* **90**, 021001 (2018).
  - [7] G. Cassabois, P. Valvin, and B. Gil, *Nat. Photon.* **10**, 262-266 (2016).
  - [8] C. Elias *et al.*, *Nat. Comm.* **10**, 2639 (2019).
  - [9] **J. Caldwell *et al.*, *Nat. Rev. Mat.* **4**, 552 (2019).**
  - [10] B. Arnaud, S. Lebègue, P. Rabiller, and M. Alouani, *Phys. Rev. Lett.* **96**, 026402 (2006).
  - [11] G. Fugallo, M. Aramini, J. Koskelo, K. Watanabe, T. Taniguchi, M. Hakala, S. Huotari, M. Gatti, and F. Sottile, *Phys. Rev. B* **92**, 165122 (2015).
  - [12] F. Pleari *et al.*, *2D Mater.* **5**, 045017 (2018).
  - [13] W. Hanke and L.J. Sham, *Phys. Rev. Lett.* **43**, 387 (1979).
  - [14] See Supplemental Material [url], which includes Refs. [15-39].
  - [15] G. Strinati, *Riv. Nuovo Cimento* **11**, 1 (1988).
  - [16] L. Hedin, *Phys. Rev.* **139**, A796 (1965).
  - [17] M. Gatti and F. Sottile, *Phys. Rev. B* **88**, 155113 (2013).
  - [18] G. Onida, L. Reining, and A. Rubio, *Rev. Mod. Phys.* **74**, 601 (2002).
  - [19] V. Olevano and L. Reining, *Phys. Rev. Lett.* **86**, 5962 (2001).
  - [20] P. Hohenberg and W. Kohn, *Phys. Rev.* **136**, B864 (1964).
  - [21] W. Kohn and L.J. Sham, *Phys. Rev.* **140**, A1133 (1965).
  - [22] N. Troullier and J. L. Martins, *Phys. Rev. B* **43**, 1993 (1991).
  - [23] X. Gonze *et al.*, *Z. Kristallogr.* **220**, 558 (2005).
  - [24] V. L. Solozhenko, G. Will, and F. Elf, *Solid State Commun.* **96**, 1 (1995).
  - [25] H. Henck *et al.* *Phys. Rev. B* **95**, 085410 (2017).
  - [26] A. Segura *et al.*, *Phys. Rev. Mat.* **2**, 024001 (2018).
  - [27] A. Marini and R. Del Sole, *Phys. Rev. Lett.* **91**, 176402 (2003).

- [28] K. Shindo, J. Phys. Soc. Jpn. **29**, 287 (1970).
- [29] F. Bechstedt, K. Tenelsen, B. Adolph, and R. Del Sole, Phys. Rev. Lett. **78**, 1528 (1997).
- [30] M. Rohlfiing and S. G. Louie, Phys. Rev. B **62**, 4927 (2000).
- [31] G. Strinati, Phys. Rev. Lett. **49**, 1519 (1982).
- [32] G. Wang *et al.*, Phys. Rev. Lett. **114**, 097403 (2015).
- [33] L. Sponza *et al.*, Phys. Rev. B **97**, 075121 (2018).
- [34] G. Cassaboïs, P. Valvin, and B. Gil, Phys. Rev. B **93**, 035207 (2016).
- [35] F. Paleari *et al.*, Phys. Rev. Lett. **122**, 187401 (2019).
- [36] T.Q.P. Vuong *et al.*, Phys. Rev. B **95**, 045207 (2017).
- [37] P. Valvin *et al.*, AIP Adv. **10**, 075025 (2020).
- [38] S. Liu *et al.*, Cryst. Growth Des. **17**, 4932-4935 (2017).
- [39] J. Li *et al.*, J. Mater. Chem. C **8**, 9931 (2020).
- [40] in *Interacting electrons theory and computational approaches*, edited by R. M. Martin, L. Reining, and D. M. Ceperley (Cambridge University Press, UK, 2016).
- [41] J. Koskelo, G. Fugallo, M. Hakala, M. Gatti, F. Sottile, and P. Cudazzo, Phys. Rev. B **95**, 035125 (2017).
- [42] S. Galambosi *et al.*, Phys. Rev. B **83**, 081413 (2011).
- [43] D.M. Hoffman, G. Doll, and P.C. Eklund, Phys. Rev. B **30**, 6051 (1984).
- [44] K. Watanabe, T. Taniguchi, and H. Kanda, Nat. Mater. **3**, 404-409 (2004).
- [45] K. Watanabe and T. Taniguchi, Phys. Rev. B **79**, 193104 (2009).
- [46] in *Fundamentals of semiconductors*, edited by P. Y. Yu and M. Cardona (Springer-Verlag, Berlin Heidelberg, 1996).
- [47] **T.Q.P. Vuong *et al.*, 2D Mater. 4, 011004 (2017).**
- [48] P.J. Dean and G.G. Thomas, Phys. Rev. **150**, 690 (1966).
- [49] Y. Kaifu and T. Komatsu, J. Phys. Soc. Japan **40**, 1377 (1976).
- [50] R. Ishii *et al.*, Jpn. J. Appl. Phys. **59**, 010903 (2019).
- [51] D. Auvergne, P. Merle, and H. Mathieu, Phys. Rev. B **12**, 1371 (1975).
- [52] L. Schué *et al.*, Phys. Rev. Lett. **122**, 067401 (2019).
- [53] in *Semiconductor optics*, edited by C. F. Klingshirn (Springer-Verlag, Berlin Heidelberg, 2007).
- [54] M.M. Denisov and V.P. Makarov, phys. stat. sol. (b) **56**, 9 (1973).
- [55] L.C. Andreani, F. Bassani, and A. Quattropani, Nuovo Cimento D **10**, 1473 (1988).
- [56] in *Physics of Wurtzite Nitrides and Oxides*, edited by B. Gil (Springer Series in Materials Science, 2014).
- [57] F. Beerwerth and D. Fröhlich, Phys. Rev. Lett. **55**, 2603-2605 (1985).
- [58] F. Beerwerth, D. Fröhlich, P. Köhler, V. Leinweber, and A. Voss, Phys. Rev. B **38**, 4250-4258 (1988).
- [59] S. Galamić-Mulaomerović and C.H. Patterson, Phys. Rev. B **72**, 035127 (2005).
- [60] R.J. Elliott, Phys. Rev. **108**, 1384-1389 (1957).
- [61] Y. Nanishi, Nat. Photon. **8**, 884-886 (2014).
- [62] M. Kneissl, T.-Y. Seong, J. Han, and H. Amano, Nat. Photon. **13**, 233-244 (2019).
- [63] **S.F. Chichibu *et al.*, J. Appl. Phys. 123, 065104 (2018).**
- [64] T.Q.P. Vuong *et al.*, Phys. Rev. B **95**, 201202 (2017).